Eur. Phys. J. D **6**, 57–62 (1999)

THE EUROPEAN
PHYSICAL JOURNAL D
EDP Sciences

Ab initio thermodynamic properties for different isomers of the Al_2O_3 molecule

A.B.C. Patzer[1], Ch. Chang[1,a], E. Sedlmayr[1], and D. Sülzle[2]

[1] Institut für Astronomie und Astrophysik, Technische Universität Berlin, Hardenbergstr. 36, D-10623 Berlin, FRG
[2] Schering AG Research Laboratories, D-13342 Berlin, FRG

Received: 9 September 1998 / Received in final form: 2 October 1998

Abstract. We present *ab initio* thermodynamic properties for seven different geometric isomers of molecular Al_2O_3 over a wide temperature range. The rigid rotator-harmonic oscillator approximation is used to calculate the partition function as it is generally applied in thermodynamic studies of polyatomic molecules. The molecular data employed in setting up the partition functions are taken from the theoretical results of *ab initio* MP2/6-31G(d) calculations. An analysis of the effects of the various contributions is made. The resulting thermodynamic functions of Al_2O_3 are consistent with the JANAF thermochemical data compilation. Some thermochemical implications are discussed.

PACS. 33.15.-e Properties of molecules and molecular ions – 82.60.-s Chemical thermodynamics

1 Introduction

Thermodynamic data are required for many investigations as, for example, the study of gas phase chemistry or also for modelling processes in stellar atmospheres. Unfortunately for many relevant molecules this information is still missing. Theoretical computation is therefore often the only means to obtain at least some estimates of the desired quantities. Among other oxygen bearing compounds molecular Al_2O_3 is a possible candidate that could be of importance in astrophysical dust formation processes (*e.g.* [1–5]); but merely data for the solid are available. Consequently, the availability of adequate thermochemical data for the Al_2O_3 molecule in the gas phase is needed not only for astrophysical applications but also, for example, for the study of evaporation processes in Al–O systems (*e.g.* [6–8]).

Ab initio studies on molecular Al_2O_3 are reported by Chang *et al.* [9], who determined fully optimised molecular geometries, normal modes, and IR intensities of possible Al_2O_3 isomers at both Hartree-Fock (HF) and second-order Møller-Plesset (MP2) levels of theory. They studied the MP2 properties of twelve isomers with seven different geometric configurations extending the former investigations ([10–13]) especially to higher spin states (see [9] for details). These *ab initio* molecular calculations were performed at the MP2 frozen core level of theory using the standard 6–31G(d) basis set. In the following the molecular data of these theoretical investigations are used to derive the thermodynamic properties for different isomers of molecular Al_2O_3 in the gas phase. Costes and Naulin [14], for example, stressed the crucial importance of the atomisation energy. In contrast to MP2 results, HF energy values show a very poor agreement with data available in the literature as discussed in detail by [9]. In consequence, the molecular data resulting from HF calculations are inappropriate to set up thermodynamic functions.

The purpose of this paper is to present thermodynamic functions of gas phase Al_2O_3 within the temperature interval of 100 K–3000 K computed from the results of MP2 *ab initio* calculations adhering rigorously to the JANAF reference system. In total seven isomeric geometric forms of Al_2O_3 are taken into consideration.

2 Thermochemistry

One should be careful, if thermodynamic data from different compilations or sources are combined, in order to avoid errors due to a lack of consistency between these tables, which are mainly caused by differences in the reference systems used (*e.g.*, reference state of the elements, standard pressure $p^{\ominus}$, or reference temperature T_0). In this paper we used the JANAF thermochemical reference system for an ideal gas at $p^{\ominus} = 1$bar and $T_0 = 298.15$K (see [15] for details). Unless otherwise specifically mentioned all values listed in the following tables were calculated using a consistent set of auxiliary data taken from the JANAF tables [15]. The resulting *ab initio* thermodynamic functions of Al_2O_3 are consistent with the JANAF data compilation.

The calculated heats of formation at $T = 0$ K, $\Delta_f H^{\ominus}(0)$, were obtained from the theoretical MP2 atomisation energies $\Delta_{at}H$ in conjunction with the standard

---

[a] e-mail: `patzer@physik.tu-berlin.de`

Table 1. Heats of formation at $\Delta_f H(0)$ / kJ mol^{-1} of the molecular Al_2O_3 isomers

^{1}**1**	^{3}**2**	^{1}**3**	^{1}**4**	^{1}**5**	^{1}**6**	^{3}**7**
−439.2	−445.0	−304.1	−236.6	−208.6	85.7	−238.5

Table 2. Structures and rotational constants of the Al_2O_3 configurations

	Structure	Group	σ	A/cm^{-1}	B/cm^{-1}	C/cm^{-1}
^{1}**1**	linear	$D_{\infty h}$	2		0.03327	
^{3}**2**	kite-shaped	C_{2v}	2	0.31556	0.08583	0.06748
^{1}**3**	Y-shaped	C_{2v}	2	0.73971	0.04387	0.04141
^{1}**4**	bipyramidal	D_{3h}	6	0.15460	0.15045	0.15045
^{1}**5**	curved	C_s	1	0.53408	0.05764	0.05561
^{1}**6**	bipyramidal	C_{2v}	2	0.24376	0.09689	0.09084
^{3}**7**	planar	C_s	1	0.30498	0.07754	0.06192

Table 3. Scaled harmonic wave numbers of seven Al_2O_3 isomers

	$\tilde{\nu}_1$/cm^{-1}	$\tilde{\nu}_2$/cm^{-1}	$\tilde{\nu}_3$/cm^{-1}	$\tilde{\nu}_4$/cm^{-1}	$\tilde{\nu}_5$/cm^{-1}
^{1}**1**	32.5	32.5	165.3	165.3	237.0
^{3}**2**	120.6	175.6	329.6	434.4	607.0
^{1}**3**	51.7	52.2	224.2	239.8	383.0
^{1}**4**	318.0	318.0	397.2	397.2	543.0
^{1}**5**	56.4	150.7	199.5	329.5	397.3
^{1}**6**	65.1	138.2	218.1	291.6	375.9
^{3}**7**	49.2	171.3	214.8	241.6	369.7

	$\tilde{\nu}_6$/cm^{-1}	$\tilde{\nu}_7$/cm^{-1}	$\tilde{\nu}_8$/cm^{-1}	$\tilde{\nu}_9$/cm^{-1}	$\tilde{\nu}_{10}$/cm^{-1}
^{1}**1**	237.0	403.5	872.2	1068.2	1170.1
^{3}**2**	645.5	714.7	744.1	890.0	
^{1}**3**	543.1	758.0	837.4	1076.7	
^{1}**4**	621.3	621.3	647.9	750.9	
^{1}**5**	468.3	570.7	737.8	1054.1	
^{1}**6**	422.0	593.6	715.7	790.1	
^{3}**7**	568.9	616.3	825.1	991.0	

experimental $\Delta_f H^\ominus(0)$ values for the neutral atoms as

$$\Delta_f H^\ominus(0) = 2\,\Delta_f H^\ominus(0)(\mathrm{Al},g) + 3\,\Delta_f H^\ominus(0)(\mathrm{O},g) \\ -\Delta_{\mathrm{at}} H \qquad (1)$$

The heats of formation of the seven different geometric Al_2O_3 isomers are listed in Table 1. The geometric structures are labelled systematically as introduced by [9]. The superscript indicates spin multiplicity g_0 of the electronic ground state. In the considered temperature range below 3000 K the excited electronic states of the different geometric configuration given in Chang *et al.* do not contribute to the electronic partition function. Therefore, the electronic part of the partition function is simply given by the degeneracy of the ground state of the isomer g_0.

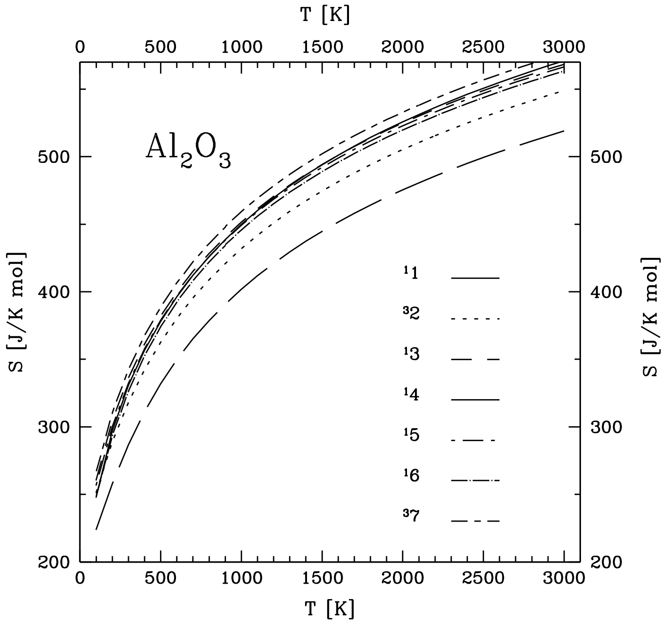

Fig. 1. Entropy of the seven isomers of molecular Al_2O_3 as a function of temperature.

Table 2 contains information about their structures such as the symmetry group, the symmetry number σ, as well as the rotational constants derived from the different principal moments of inertia. The vibrational wave numbers scaled by 0.9434 (cf. [16]) are tabulated in Table 3.

The rigid rotator-harmonic oscillator (RRHO) approximation is used to set up the partition function as it is generally applied in thermodynamic studies of polyatomic molecules. The different contributions to the partition function were evaluated separately. From the partition function Q the thermodynamic functions can easily be calculated by standard statistics as described by,*e.g.*, [17,18]. In thermochemical calculations the entropy S is an absolute quantity, whereas enthalpy changes are relative quantities in the chosen standard reference system. $\Delta_f H^\ominus(T)$ represents the standard enthalpy of formation, which is the enthalpy change associated with the reaction of forming Al_2O_3 from its elements in their *reference states.* The Gibbs energy of formation $\Delta_f G^\ominus$ can simply be determined from S and $\Delta_f H^\ominus$, when the entropies of the elements in their reference states are known.

According to the JANAF style we calculated these thermodynamic functions from 100 K to 3000 K temperature range in increments of 100 K. Our program was tested by reproducing the JANAF data tables of the linear Al_2O and AlO_2 molecules, and the planar species $(AlO)_2$ with the molecular constants given in [15].

3 Results and discussion

Figure 1 presents the entropy of the seven Al_2O_3 isomers as a function of temperature. Surprisingly four configurations have nearly the same entropy values caused by

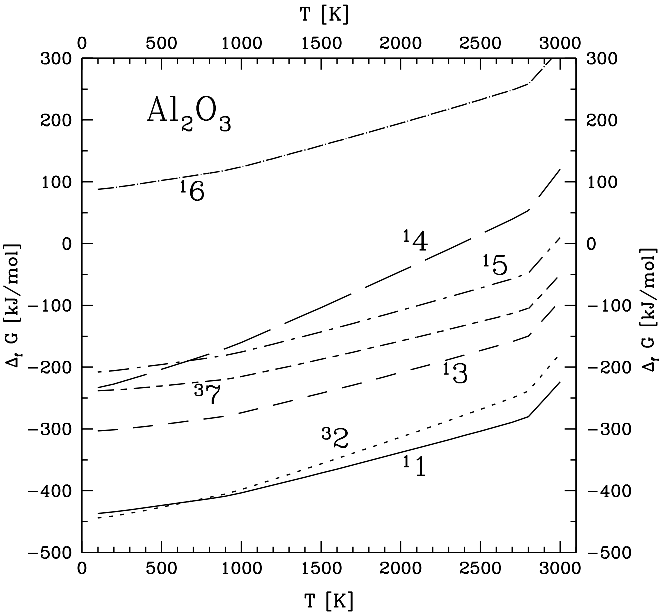

Fig. 2. Gibbs free energy of formation $\Delta_f G^{\ominus}(T)$ of the Al_2O_3 isomers.

partition functions of comparable size. The products of the rotational and of the vibrational partition functions of the Y-shaped isomer $^1\mathbf{3}$, of the curved structure $^1\mathbf{5}$, and of bipyramidal $^1\mathbf{6}$ are approximately equal. The remarkable smaller rotational part of the partition function of linear $^1\mathbf{1}$ is compensated by the large vibrational contribution to its partition function. Consequently the partition functions of $^1\mathbf{1}$, $^1\mathbf{3}$, $^1\mathbf{5}$, and $^1\mathbf{6}$, and therefore their entropies, are nearly equal. Only the entropy of the kite-shaped isomer $^3\mathbf{2}$ and of bipyramidal $^1\mathbf{4}$ deviate substantially, an effect, which increases with higher temperatures (cf. Fig. 1). Their vibrational parts contribute only modestly to the partition functions compared with the other isomers. In addition $Q_{\rm rot}$ of $^1\mathbf{4}$ is noticeably smaller than $Q_{\rm rot}$ of $^3\mathbf{2}$. Planar $^3\mathbf{7}$ has the highest entropy of all configurations caused by its large partition function, to which the rotational part is the main contribution.

In contrast to the entropy S, which is a smooth function, the Gibbs energy of formation $\Delta_f G^{\ominus}$ has discontinuities reflecting to the phase transition temperatures in the reference state of the element aluminum, whereas the reference state of oxygen is represented by a single phase. These discontinuous changes are noticeable in Figure 2 depicting the $\Delta_f G^{\ominus}$ of the molecular Al_2O_3 isomers as functions of temperature. The solid/liquid transition of Al(ref) at $T = 933.450$ K as well as its liquid/gas transition at $T = 2790.812$ K can clearly be seen.

The temperature dependence of $\Delta_f G^{\ominus}$ of $^1\mathbf{1}$, $^1\mathbf{3}$, $^1\mathbf{5}$, and $^1\mathbf{6}$ is roughly the same caused by their almost equal partition functions. Considering the differences in the $\Delta_f G^{\ominus}$ data at $T = 0$ K and at $T = 3000$ K the deviations between these isomers are less than 10%. Thus, these thermodynamic functions differ mainly due to the differences in their $\Delta_f H^{\ominus}(0)$ values. In contrast the temperature dependence of the Gibbs free energies of formation of $^3\mathbf{2}$ and of $^1\mathbf{4}$ are completely different, which leads to a point of intersection between $^1\mathbf{4}$ and $^1\mathbf{5}$ at $T \approx 670$ K. This means that despite of its 28 kJ/mol lower atomisation energy the curved structure becomes more "favourable" at higher temperatures than the bipyramidal isomer caused by the influence of the entropy term, which increases with rising temperature. The different temperature behaviour of $^3\mathbf{2}$ and of $^1\mathbf{1}$ leads also to a point of intersection between their two $\Delta_f G^{\ominus}$ curves (Fig. 2). Below ca. 680 K the C_{2v} triplet $^3\mathbf{2}$ has the lowest Gibbs energy of formation of all Al_2O_3 isomers, but at high temperatures, the most stable isomer is undoubtedly the linear molecule $^1\mathbf{1}$. *Ab initio* thermodynamic properties of these two energetically lowest Al_2O_3 structures are explicitly listed in Appendix (Tabs. 4, 5).

4 Application

The availability of thermodynamic functions for molecular systems, such as presented in Tabs. 4 and 5, is of determinative importance for the calculation of multicomponent gas phase equilibria. If a gaseous system at temperature T and pressure P consisting of, for instance, N_S elements $A, B, C, \cdots, S$ is envisaged, then by the law of mass conservation and the condition that the Gibbs free energy is minimal at equilibrium,

$$(dG)_{T,P} = 0 \tag{2}$$

a system of N_S in general highly nonlinear algebraic equations is obtained (see, *e.g.*, [19]):

$$P_{\langle M\rangle} = \sum_{\nu_A,\cdots,\nu_S=0}^{\infty} \nu_M K^{\rm dis}_{A_{\nu_A}\cdots S_{\nu_S}} p^{\ominus\left[1-\sum_{i=A}^{S}\nu_i\right]} \prod_{i=A}^{S} P_i^{\nu_i}, \tag{3}$$

where $P_{\langle M\rangle}$ is an assumed overall pressure of element M accruing from all possible dissociative molecular contributions, the indices $\nu_A, \nu_B, \cdots, \nu_S$ respectively are the stoichiometric coefficients of the elements $A, B, C, \cdots, S$ in every molecular species $A_{\nu_A} B_{\nu_B} \cdots S_{\nu_S}$, $p^{\ominus}$ is again the standard pressure, and $K^{\rm dis}_{A_{\nu_A} B_{\nu_B} \cdots S_{\nu_S}}$ are the dissociation constants for each molecular formation process from the state of completely separated atoms. Thus, the partial pressure of a molecule $A_{\nu_A} B_{\nu_B} \cdots S_{\nu_S}$ is given by

$$P_{A_{\nu_A} B_{\nu_B} \cdots S_{\nu_S}} = K^{\rm dis}_{A_{\nu_A} B_{\nu_B} \cdots S_{\nu_S}} p^{\ominus\left[1-\sum_{i=A}^{S}\nu_i\right]} \prod_{i=A}^{S} P_i^{\nu_i}. \tag{4}$$

Given $P^{\rm dis} = P_{\langle A\rangle} + P_{\langle B\rangle} + \cdots + P_{\langle S\rangle}$, thereby fixing the total amount of each atomic species $A, B, \cdots, S$ and all dissociation constants $K^{\rm dis}$, the system of equations can be solved numerically to yield the equilibrium distribution of partial pressures of all comprised species as a function of temperature. This way to formulate a gas phase equilibrium is consummately general, because any equilibrium constant K of any chemical reaction among the species in the system can be expressed in terms of the constants $K^{\rm dis}$.

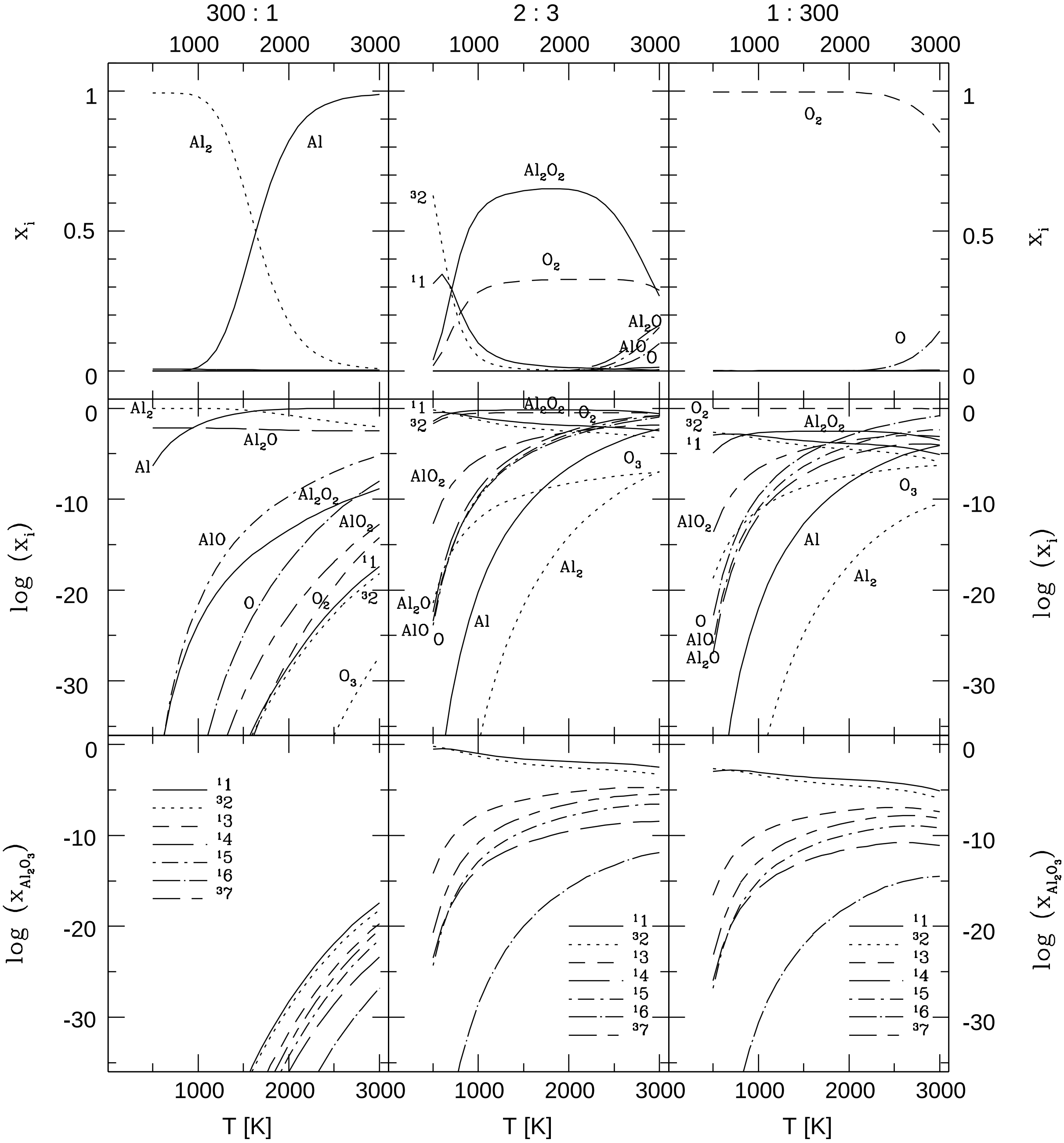

Fig. 3. Abundances $x_i = P_i/P$ for the Al/O system for different stoichiometric ratios λ vs. temperature.

We used the above approach to calculate the gas phase equilibrium of the system Al/O. As there are only two atomic species involved the system equation (3) consists of just two equations. In the summations only those terms for which the thermochemical data can be found in the literature [15] and the seven stable isomers of Al_2O_3 from our present work were included. A pressure $P^{\text{dis}} = p^{\varpi} = 1\text{bar}$ and three different ratios of $\lambda = (P_{\langle \text{Al} \rangle}/P_{\langle \text{O} \rangle})$, namely $\lambda = (1/300)$, $(2/3)$, which is the stoichiometric ratio in solid Al_2O_3, and $(300/1)$ were chosen. The temperature dependent results are illustrated in Figure 3.

The linearly scaled plot (upper three panels) shows for large excess aluminium (oxygen), *i.e.* $\lambda \gg 1$ ($\lambda \ll 1$), that the most prominent molecular species is Al_2 (O_2), as expected. Rising the temperature both molecules are dissociated, but because Al_2 is less strongly bound, its abundance falls off at lower temperatures ($T > 1000$ K) than that of O_2, which decreases at temperatures above $T \approx 2500$ K. When $\lambda = 2/3$, *i.e.* there is just slightly more oxygen than aluminium available, the situation is conspicuously different. Here over a wide temperature range (750 – 2500 K) Al_2O_2 is the dominant aluminium oxide. At temperatures < 750K, however, the two most stable isomers of Al_2O_3, *viz.* $^1\mathbf{1}$ and $^3\mathbf{2}$, rise significantly in abundance.

The same can be inferred from the middle three panels, but as the abundance scale is now logarithmic, the behaviour of the other species in the system becomes discernible. If $\lambda \gg 1$ next to the Al_2 diatomic, Al_2O is the

Table 4. Thermodynamic functions of the linear Al_2O_3 molecule $^1\mathbf{1}$.

T K	S J $K^{-1}mol^{-1}$	$(G(T)-H(T_0))/T$ J K^{-1} mol^{-1}	$H(T)-H(T_0)$ kJ mol^{-1}	$\Delta_{\mathrm{f}}H^{\ominus}$ kJ mol^{-1}	$\Delta_{\mathrm{f}}G^{\ominus}$ kJ mol^{-1}
100	247.6	401.6	−15.4	−439.7	−437.0
200	297.2	338.0	−8.2	−440.4	−434.1
300	330.8	330.3	0.2	−441.1	−430.8
400	356.8	333.8	9.2	−441.5	−427.4
500	378.1	340.6	18.8	−441.8	−423.8
600	396.3	348.4	28.8	−442.0	−420.2
700	412.1	356.4	39.0	−442.3	−416.5
800	426.1	364.2	49.5	−442.8	−412.8
900	438.6	371.8	60.1	−443.6	−409.0
1000	449.8	379.1	70.8	−465.9	−403.6
1100	460.1	386.0	81.6	−466.7	−397.3
1200	469.6	392.6	92.4	−467.6	−391.0
1300	478.3	398.8	103.4	−468.4	−384.6
1400	486.4	404.8	114.3	−469.2	−378.1
1500	494.0	410.5	125.3	−470.0	−371.6
1600	501.1	415.9	136.3	−470.8	−365.0
1700	507.8	421.1	147.4	−471.7	−358.3
1800	514.2	426.1	158.4	−472.5	−351.7
1900	520.1	430.9	169.5	−473.4	−344.9
2000	525.8	435.5	180.6	−474.3	−338.1
2100	531.3	440.0	191.7	−475.2	−331.3
2200	536.4	444.2	202.8	−476.2	−324.4
2300	541.4	448.4	213.9	−477.2	−317.5
2400	546.1	452.3	225.1	−478.2	−310.5
2500	550.7	456.2	236.2	−479.2	−303.5
2600	555.0	459.9	247.4	−480.2	−296.5
2700	559.2	463.5	258.5	−481.3	−289.4
2800	563.3	467.0	269.7	−1070.2	−280.3
2900	567.2	470.4	280.8	−1069.1	−252.1
3000	571.0	473.7	292.0	−1068.1	−224.0

second most prevailing species over the whole temperature range. Yet, by about two orders of magnitude lower. If $\lambda \ll 1$ the behaviour of the oxide species is somewhat comparable to the situation at $\lambda = 2/3$ shifted by about $3-4$ orders of magnitude downwards, due to the universal presence of O_2. Furthermore at higher temperatures ($T > 2500$ K) another oxide, AlO, becomes important.

From the lower three panels showing in detail the seven Al_2O_3 isomers, it can be concluded, that apart from the two most stable of them, $^1\mathbf{1}$ and $^3\mathbf{2}$, all others have negligibly small abundances over the complete temperature range for any ratio λ. However, the overabundance of Al has a decisive influence on the formation of molecular Al_2O_3, because a large excess of aluminium suppresses the formation almost totally (cf. lower panel, $\lambda = 300/1$).

5 Concluding remarks

The results presented in this study indicate that the derived thermodynamic properties for the different configurations of the Al_2O_3 molecule in the gas phase led to the conclusion that the symmetrical linear structure $^1\mathbf{1}$ as well as the triplet structure $^3\mathbf{2}$ of planar C_{2v} symmetry are the main isomers of this system, as also confirmed by the obtained results of multicomponent gas phase equilibrium calculations. Our results establish that both molecular forms are expected to be detectable among the reaction products in, for example, experiments generating the Al_xO_y system in inert gas matrices at low temperatures (cf., *e.g.*, [12]).

Furthermore it becomes evident that it can be important to consider separately the thermodynamic properties of different stable isomers. At least in situations where the molecular system under consideration gives rise to many different energetically similar stable species as it is the case for molecular Al_2O_3. If the molecular quantities to derive these thermodynamic functions are not or just insufficiently at hand from experimental sources, then *ab initio* theoretical techniques provide a reasonable way to obtain the required data.

All calculations have been performed on the SGI cluster of the Institut für Astronomie und Astrophysik, TU Berlin. The authors are grateful to T.U. Arndt for his support on text processing adaptations.

Appendix

The thermochemical tables for $^1\mathbf{1}$ and $^3\mathbf{2}$ consist of thermal functions (entropy S, enthalpy increments

Table 5. Thermodynamic functions of the Al_2O_3 triplet $^3\mathbf{2}$.

T K	S J $K^{-1}mol^{-1}$	$(G(T) - H(T_0))/T$ J K^{-1} mol^{-1}	$H(T) - H(T_0)$ kJ mol^{-1}	$\Delta_f H^{\ominus}$ kJ mol^{-1}	$\Delta_f G^{\ominus}$ kJ mol^{-1}
100	251.2	377.6	−12.6	−446.4	−444.2
200	289.2	324.5	−7.1	−448.8	−441.0
300	318.2	317.7	0.1	−450.6	−436.6
400	342.3	321.0	8.5	−451.7	−431.8
500	362.7	327.3	17.7	−452.4	−426.7
600	380.2	334.7	27.3	−453.0	−421.5
700	395.4	342.3	37.2	−453.7	−416.2
800	408.9	349.8	47.3	−454.5	−410.8
900	421.0	357.1	57.5	−455.7	−405.3
1000	431.9	364.0	67.9	−478.3	−398.1
1100	441.9	370.6	78.3	−479.5	−390.0
1200	451.0	377.0	88.8	−480.7	−381.8
1300	459.4	383.0	99.4	−481.9	−373.5
1400	467.3	388.7	110.0	−483.0	−365.1
1500	474.6	394.2	120.6	−484.2	−356.7
1600	481.5	399.5	131.2	−485.5	−348.1
1700	487.9	404.5	141.9	−486.7	−339.5
1800	494.0	409.3	152.5	−488.0	−330.8
1900	499.8	413.9	163.2	−489.2	−322.1
2000	505.3	418.3	173.9	−490.5	−313.2
2100	510.5	422.6	184.6	−491.8	−304.4
2200	515.5	426.7	195.3	−493.2	−295.4
2300	520.3	430.7	206.1	−494.6	−286.4
2400	524.9	434.6	216.8	−496.0	−277.4
2500	529.3	438.3	227.5	−497.4	−268.3
2600	533.5	441.9	238.3	−498.8	−259.1
2700	537.6	445.3	249.0	−500.3	−249.9
2800	541.5	448.7	259.8	−1089.6	−238.7
2900	545.3	452.0	270.5	−1089.0	−208.3
3000	548.9	455.2	281.3	−1088.3	−178.0

$[H(T) - H(T_0)]$, and Gibbs energy function $[G(T) - H(T_0)]/T)$ and formation functions (enthalpy of formation $\Delta_f H^{\ominus}$, and the Gibbs energy of formation $\Delta_f G^{\ominus}$), which all are temperature dependent.

References

1. T. Kozasa, H. Hasegawa, Prog. Theor. Phys. **77**, 1402 (1987).
2. E. Sedlmayr, in *Interstellar Dust, IAU Symp. No. 135*, edited by L.J. Allamandola, A.G.G.M. Tielens (Kluwer, Dordrecht, 1989), p. 467-477.
3. A.G.G.M. Tielens, in *From Miras to Planetary Nebulae: Which path for stellar evolution?*, edited by M.O. Mennessier, A. Omont (Éditions Frontières, Gif sur Yvette, 1990), p. 186-200.
4. B. Begemann, J. Dorschner, T. Henning, H. Mutschke, J. Gürtler, C. Kömpe, R. Nass, Astrophys. J. **476**, 199 (1997).
5. L.R. Nittler, C.M.O.D. Alexander, X. Gao, R.M. Walker, E. Zinner, Astrophys. J. **483**, 475 (1997).
6. R.P. Burns, J. Chem. Phys. **44**, 3307 (1966).
7. C.B. Alcock, M. Peleg, Trans. Brit. Ceram. Soc. **66**, 217 (1967).
8. H. Yanagida, F.A. Kröger, J. Am. Ceram. Soc. **51**, 700 (1968).
9. Ch. Chang, A.B.C. Patzer, E. Sedlmayr, D. Sülzle, Eur. Phys. J. D **2**, 57 (1998).
10. V.G. Solomonik, V.V. Sliznev, Russ. J. Inorg. Chem. **32**, 788 (1987).
11. A.V. Nemukhin, F. Weinhold, J. Chem. Phys. **97**, 3420 (1992).
12. L. Andrews, T.R. Burkholder, J.T. Yustein, J. Phys. Chem. **96**, 10182 (1992).
13. S.R. Desai, H. Wu, C.M. Rohlfing, L.S. Wang, J. Chem. Phys. **106**, 1309 (1997).
14. M. Costes, C. Naulin, in *Molecules in the Stellar Environment, Proc. IAU Coll. No. 146*, edited by U.G. Jørgensen (Springer, Berlin, 1994), p. 250-264.
15. M.W. Chase Jr., C.A. Davies, J.R. Downey Jr., D.J. Frurip, R.A. McDonald, A.N. Syverud, J. Phys. Chem. Ref. Data **14** Suppl. **1**, National Bureau of Standards (1985).
16. J.B. Foresman, E. Frisch, *Exploring Chemistry with Electronic Structure Methods* (Gaussian Inc., Pittsburgh PA, 1996).
17. T.L. Hill, *An Introduction to Statistical Thermodynamics* (Dover, New York, 1986).
18. P.W. Atkins, *Physical Chemistry* (Oxford Univ. Press, Oxford, 1990).
19. H.N. Russell, Astrophys. J. **79**, 317 (1934).